2lp

N63-15235

NASA TN D-1776

Code-1

NASA TN D-1776

TECHNICAL NOTE

D-1776

AERODYNAMIC CHARACTERISTICS OF A FLEXIBLE-CANOPY PARAGLIDER MODEL AT A MACH NUMBER OF 4.5 FOR ANGLES OF ATTACK TO 360° AND SIDESLIP ANGLES FROM 0° TO 90°

By Dewey E. Wornom and Robert T. Taylor

Langley Research Center
Langley Station, Hampton, Va.

NATIONAL AERONAUTICS AND SPACE ADMINISTRATION

WASHINGTON April 1963

34p 554242

NATIONAL AERONAUTICS AND SPACE ADMINISTRATION

TECHNICAL NOTE D-1776

AERODYNAMIC CHARACTERISTICS OF A FLEXIBLE-CANOPY PARAGLIDER MODEL AT A MACH NUMBER OF 4.5 FOR ANGLES OF ATTACK TO 360° AND SIDESLIP ANGLES FROM 0° TO 90°

By Dewey E. Wornom and Robert T. Taylor

SUMMARY

15235

Force tests of a flexible-canopy paraglider model with a rigid frame have been conducted at a Mach number of 4.5 in the 2-foot hypersonic facility at the Langley Research Center. The aerodynamic characteristics were measured over an angle-of-attack range from 0° to 360° for sideslip angles from 0° to 90° at a Reynolds number of approximately 0.3×10^6 based on a model keel length of 5.75 inches. The variation of the aerodynamic coefficients with angle of attack at constant sideslip angles are presented with limited discussion.

For the moment reference center selected, the data at zero sideslip showed that longitudinal trim occurred at an angle of attack of 45.5° with a corresponding lift coefficient of 0.45 and a lift-drag ratio of 0.94. A maximum lift coefficient of 0.79 was obtained at an angle of attack of 68°. From visual observations of canopy action during the tests abrupt load reversal was noted to occur around an angle of attack of 180°.

INTRODUCTION

Application of the inflatable-paraglider concept as a recovery device for expended booster rockets and casings, manned spacecraft, and instrument payloads from orbital or suborbital flight has been considered by the Langley Research Center. Both experimental and analytical investigations have been conducted to evaluate the capabilities of the paraglider as such a device; results of these studies have been reported in references 1 to 6.

When recovery of instrumented space experiments using an uncontrolled paraglider is contemplated, it must be determined whether the paraglider will enter the atmosphere satisfactorily regardless of initial attitude. In addition to these studies of the paraglider dynamics on entry, a knowledge of aerodynamic heating and of loads is required. Definition of the static aerodynamic characteristics of the flight vehicle is a first step in any such study.

The purpose of this present investigation was to obtain the static aerodynamic characteristics of a proposed 0.0472-scale paraglider configuration, designed for recovery of an instrument package. Force tests of the paraglider model with a flexible canopy on a rigid frame were conducted at a Mach number of 4.5 up to an angle of attack of 360° for sideslip angles from 0° to 90°.

SYMBOLS

The forces and moments are referred to the body axis system. (See fig. 1.) In addition, lift and drag are also presented at zero sideslip. The moment reference center was located 58.33 percent of the theoretical model length aft of the intersection of the center lines of the leading-edge tubes and 50 percent of the theoretical model length below the center line of the keel tube. (See fig. 2.)

b span of canopy, 8.49 in.

C_A axial-force coefficient, $\frac{\text{Axial force}}{qS}$

C_D drag coefficient, $\frac{\text{Drag}}{qS}$

C_L lift coefficient, $\frac{\text{Lift}}{qS}$

C_N normal-force coefficient, $\frac{\text{Normal force}}{qS}$

C_m pitching-moment coefficient,
$$\frac{\text{Pitching moment about moment reference center}}{qSl}$$

C_n yawing-moment coefficient,
$$\frac{\text{Yawing moment about moment reference center}}{qSb}$$

C_Y side-force coefficient, $\frac{\text{Side force}}{qS}$

C_l rolling-moment coefficient,
$$\frac{\text{Rolling moment about moment reference center}}{qSb}$$

l theoretical length of model, 6.00 in.

L/D lift-drag ratio

M free-stream Mach number

q free-stream dynamic pressure, lb/sq ft

S canopy area, $bl/2$, 0.177 sq ft

α angle of attack, deg

β angle of sideslip, deg

γ vertical angular displacement of model support arm relative to tunnel center line, deg (see fig. 3)

ϕ lateral angular displacement of model support arm relative to vertical plane through tunnel center line, deg (see fig. 3)

APPARATUS AND MODEL

The investigation was conducted in the 2-foot hypersonic facility at the Langley Research Center. This facility is a continuous-flow low-density variable Mach number tunnel. A description of this facility is given in reference 7.

A schematic diagram of the model support system is shown in figure 3 and photographs of the model installed in the tunnel are presented as figure 4. Fixed values of ϕ were obtained by inserting angled adapters in the model support arm and γ was varied by revolving the rotating side plate. This support system maintained the model in the center of the tunnel over the complete angle ranges of the investigation.

For the model forward condition the model support arm entered the model at the base of the keel tube (fig. 4(a)) and for the model reversed condition the model support arm entered at the nose of the model with a semispherical plug being inserted in the base of the keel tube (fig. 4(b)). Since considerable difficulty was experienced in maintaining an undamaged canopy, two interchangeable models were used to expedite the tests. Extreme care was exercised in attaching the replacement canopies to the leading-edge and keel tubes of the two models to assure identical canopy shape since any difference would alter the forces and moments measured.

Dimensional details of the 0.0472-scale model, including canopy development, are given in figure 2. The leading-edge, keel, and payload support tubes were integrally molded of plastic with metal inserts for strength. The canopy, made of 3.8-ounce dacron sailcloth, was attached to the leading-edge tubes with cement and held securely on top of the keel tube by a 0.05-inch-thick metal plate. The trailing edge of the canopy was folded twice and stitched for strength as shown in sketch 1.

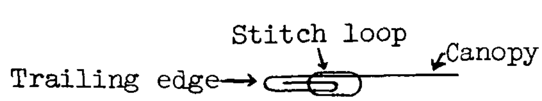

Sketch 1

Several differences between the model and a full-scale paraglider exist: The full-scale vehicle would have shroud lines from the leading-edge tube to the bottom of the payload support tube, whereas on the model for these tests the lines were not present; the keel tube of the full-scale vehicle would be tapered like the leading-edge tubes; and, since a balance and model support arm had to enter the base of the model keel tube, it was necessary to make this tube a constant diameter.

TESTS, MEASUREMENTS, AND ACCURACY

Tests were conducted at a Mach number of 4.5 with a stagnation pressure of about 2,120 pounds per square foot absolute, a stagnation temperature of about 300° F, and a Reynolds number of approximately 0.3×10^6 based on a model keel length of 5.75 inches.

To obtain the angle-of-attack range from 0° to 360°, the model support arm was varied from $\gamma = -90^\circ$ (or 270°) to 90° with the model facing forward (fig. 4(a)) and then facing rearward (fig. 4(b)). To obtain the sideslip range from 0° to 90°, values of ϕ of 0°, 10°, 30°, 60°, 87°, and 90° were used for both model forward and model reversed on the support system. The actual angles of attack and sideslip were computed from the set values of γ and ϕ by the following equations:

$$\alpha = \tan^{-1}\left(\frac{\tan \gamma}{\cos \phi}\right)$$

$$\beta = \sin^{-1}(\sin \phi \cos \gamma)$$

Forces and moments were measured by an internally cooled (water) six-component electrical strain-gage balance mounted within the keel tube of the model. The measured coefficients are estimated to be accurate within the following limits:

C_N	±0.030
C_A	±0.010
C_m	±0.015
C_l	±0.001
C_n	±0.010
C_Y	±0.025

Angular measurements were corrected for balance and model support deflections under load. The angles of attack and sideslip were estimated to be within ±0.2°.

Calibrations of the tunnel test section indicate that local deviations from the average free-stream Mach number in the region of the model were of the order of ±0.03. The average free-stream Mach number was held to within ±0.02 of the nominal value of 4.5.

The effects of the presence of the model support system were not determined during these tests and no corrections have been applied to the presented data to account for support interference. The data have not been corrected for base or balance-chamber pressure.

RESULTS AND DISCUSSION

Aerodynamic Data

The basic data for a Mach number of 4.5 are presented in table I. The discrepancies between overlapping data in these tables may be due either to the difference in support interference resulting from reversing the model on the model support arm or to the possible differences in canopy shape resulting from replacing canopies on the models or to both.

The basic data of table I were cross-plotted to obtain the variation of the force and moment coefficients with angle of attack at constant values of sideslip angle. The results of the cross-plotting are presented in figure 5. Because of the manner in which the variations in angle of attack and sideslip angle were accomplished by the model support system and because of the number of test points taken over the large angle range of these tests, there were areas of insufficient data points to define the cross-plotted data. These insufficiently defined areas are indicated by the dashed lines in figure 5; however, data listed in table I(f) fully define the force and moment coefficients at $\alpha = 90^\circ$ and 270°. The discontinuity of the curves at an angle of attack of 180° coincides with the observed abrupt reversal of canopy loading that occurred approximately at that point. Since this reversal of loading was damaging to the canopy, no attempt was made to define the actual angle of attack where the reversal occurred.

The longitudinal aerodynamic characteristics of the paraglider model are presented in figure 6. For the moment reference center selected the model was longitudinally stable at angles of attack greater than 20°. Longitudinal trim occurred at an angle of attack of 45.5° ($C_L = 0.45$) with a corresponding lift-drag ratio of 0.94, which was essentially the maximum value obtainable. A maximum lift coefficient of approximately 0.79 was reached at an angle of attack of around 68°.

Canopy Action

Visual observation of the canopy during the tests showed that at 0° angles of attack and sideslip the canopy lay between the leading-edge and keel tubes and began to fill out slowly as the angle of attack was increased. (See sketch 2.) At $\alpha = 20^\circ$ and up to 20.5° the canopy appeared to be completely

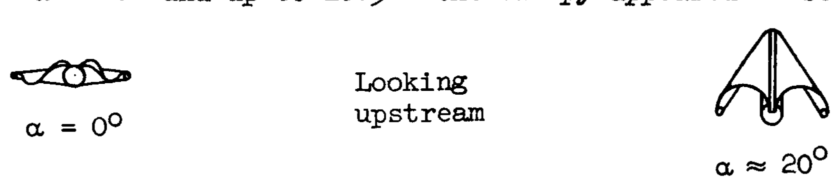

Sketch 2

filled out but the trailing edge fluttered violently. At higher angles of attack the canopy became steady and completely loaded positively. The canopy action around $\alpha = 20^{\circ}$ occurred without hysteresis and is related to the longitudinal aerodynamic characteristics of the model in figure 6. The smooth variation of lift coefficient with angle of attack around $\alpha = 20^{\circ}$ indicates that there was no sudden loading of the canopy. The change in slope of the pitching-moment-coefficient curve from an unstable slope below $\alpha = 20^{\circ}$ to a stable slope above this angle of attack shows that the canopy loading is contributing a stabilizing force to the complete model. Above $\alpha = 90^{\circ}$ the complete exposure of the canopy trailing edge to the oncoming airstream caused the trailing edge to buckle with ripples running parallel to the trailing edge. This condition became more severe as the angle of attack was increased to 180°. It was also noted during the tests that for the angle-of-attack range from 90° to 180° extreme stress appeared to be imposed upon the canopy near the nose of the model between the leading-edge and keel tubes, which was caused by the oncoming airstream being trapped in this region. As previously mentioned, canopy load reversal occurred around $\alpha = 180^{\circ}$ with the canopy being fully loaded and smooth until it unloaded gently at $\alpha = 330^{\circ}$; the canopy then slowly collapsed to the previous condition stated for $\alpha = 0^{\circ}$.

In general, the effect of sideslip on the canopy action was to require higher angles of attack to completely load the canopy in a symmetrical shape due to the cross flow of air. For some model attitudes this cross flow caused the upstream panel of the canopy to flutter violently and occasionally caused the trailing-edge stitching to unravel.

CONCLUSIONS

Results of force tests of a flexible-canopy paraglider model at a Mach number of 4.5 up to an angle of attack of 360° for sideslip angles from 0° to 90° indicate the following conclusions:

1. For the moment center selected longitudinal trim occurred at an angle of attack of 45.5° with a corresponding lift coefficient of 0.45 and a lift-drag ratio of 0.94.

2. A maximum lift coefficient of approximately 0.79 occurred at an angle of attack of around 68°.

3. Abrupt canopy load reversal was noted to occur around an angle of attack of 180°.

Langley Research Center,
National Aeronautics and Space Administration,
Langley Station, Hampton, Va., January 28, 1963.

REFERENCES

1. Rogallo, Francis M., Lowry, John G., Croom, Delwin R., and Taylor, Robert T.: Preliminary Investigation of a Paraglider. NASA TN D-443, 1960.

2. Fournier, Paul G., and Bell, B. Ann: Low Subsonic Pressure Distributions on Three Rigid Wings Simulating Paragliders With Varied Canopy Curvature and Leading-Edge Sweep. NASA TN D-983, 1961.

3. Taylor, Robert T.: Wind-Tunnel Investigation of Paraglider Models at Supersonic Speeds. NASA TN D-985, 1961.

4. Hatch, Howard G., Jr., and McGowan, William A.: An Analytical Investigation of the Loads, Temperatures, and Ranges Obtained During the Recovery of Rocket Boosters by Means of a Parawing. NASA TN D-1003, 1962.

5. Fournier, Paul G., and Bell, B. Ann: Transonic Pressure Distributions On Three Rigid Wings Simulating Paragliders With Varied Canopy Curvature and Leading-Edge Sweep. NASA TN D-1009, 1962.

6. Penland, Jim A.: A Study of the Aerodynamic Characteristics of a Fixed Geometry Paraglider Configuration and Three Canopies With Simulated Variable Canopy Inflation at a Mach Number of 6.6. NASA TN D-1022, 1962.

7. Stokes, George M.: Description of a 2-Foot Hypersonic Facility at the Langley Research Center. NASA TN D-939, 1961.

TABLE I.- BASIC AERODYNAMIC DATA AT $M = 4.5$

(a) $\phi = 0^{\circ}$

α, deg	β, deg	C_N	C_A	C_m	C_l	C_n	C_Y
Model forward							
2.4	0.0	0.02	0.18	0.062	0.002	-0.00	0.007
5.0	.0	.04	.18	.064	.002	-.00	.008
7.5	.0	.05	.18	.067	.001	-.00	.006
10.0	.0	.07	.18	.070	.001	-.00	.004
15.0	.0	.11	.19	.077	-.001	-.00	-.002
20.0	.0	.16	.18	.078	.000	-.00	.002
25.1	.0	.22	.17	.073	.000	-.00	.002
30.1	.0	.31	.15	.067	.000	-.00	-.000
35.2	.0	.40	.11	.049	-.005	-.00	-.012
40.2	.0	.53	.08	.032	-.001	-.00	-.004
45.3	.0	.65	.01	-.002	-.006	-.00	-.014
50.4	.0	.80	-.03	-.028	-.005	-.00	-.010
55.4	.0	.94	-.14	-.085	-.011	-.00	-.025
60.5	.0	1.07	-.23	-.128	-.012	-.00	-.026
70.6	.0	1.29	-.38	-.179	-.012	-.00	-.023
80.7	.0	1.32	-.49	-.229	-.018	-.00	-.035
90.8	.0	1.34	-.51	-.195	-.024	-.02	.005
Model reversed							
88.9	0.0	1.43	-0.57	-0.251	0.007	-0.01	0.050
109.2	.0	.86	-.34	-.271	-.010	-.00	.009
128.9	.0	1.25	-.74	-.456	-.002	.00	-.013
139.0	.0	1.11	-.68	-.402	.008	.00	.018
149.1	.0	1.01	-.68	-.402	.008	.00	.016
159.2	.0	.88	-.68	-.390	.005	-.00	.017
169.4	.0	.72	-.64	-.352	.003	-.00	.020
179.5	.0	.55	-.58	-.302	.001	-.00	.025
190.3	.0	-.45	-.36	-.150	.001	.00	.005
200.6	.0	-.77	-.41	-.172	-.001	.00	.003
210.8	.0	-1.02	-.44	-.182	-.003	.00	-.000
220.9	.0	-1.11	-.42	-.143	-.003	.00	.002
230.9	.0	-1.20	-.39	-.141	-.005	.00	.002
251.0	.0	-1.34	-.34	-.149	-.008	.00	-.009
271.0	.0	-1.39	-.29	-.164	-.008	.00	-.007
Model forward							
269.3	0.0	-1.35	-0.27	-0.145	0.002	-0.00	0.003
279.2	.0	-1.35	-.23	-.142	.002	-.00	.004
289.2	.0	-1.32	-.19	-.131	.003	-.00	.006
299.3	.0	-1.24	-.13	-.081	.002	-.00	.004
309.5	.0	-.89	-.03	-.033	.001	-.00	.002
319.6	.0	-.56	.05	.004	.000	-.00	.001
329.8	.0	-.33	.09	.018	.000	-.00	.003
334.8	.0	-.22	.11	.028	-.000	-.00	.000
349.9	.0	-.05	.14	.039	-.001	-.00	-.000
352.4	.0	-.00	.17	.055	-.001	-.00	-.001
354.9	.0	-.01	.15	.045	-.000	-.00	.001
357.4	.0	.01	.16	.048	-.002	-.00	-.002
359.9	.0	.01	.18	.060	.003	-.00	.009

TABLE I.- BASIC AERODYNAMIC DATA AT M = 4.5 - Continued

(b) $\phi = 10^{\circ}$

α, deg	β, deg	C_N	C_A	C_m	C_l	C_n	C_Y
Model forward							
5.0	9.9	0.04	0.19	0.067	-0.017	0.00	-0.060
7.6	9.9	.05	.19	.069	-.019	.00	-.061
10.1	9.8	.07	.19	.072	-.019	.00	-.060
12.7	9.7	.08	.19	.075	-.020	.00	-.062
15.2	9.6	.10	.19	.076	-.021	.00	-.064
17.8	9.5	.13	.19	.082	-.025	.00	-.072
20.3	9.3	.16	.19	.084	-.026	.00	-.074
25.4	9.0	.22	.18	.079	-.026	.00	-.074
30.5	8.6	.31	.15	.070	-.028	.00	-.078
35.6	8.1	.39	.12	.059	-.032	.00	-.084
40.7	7.6	.52	.08	.037	-.035	.00	-.088
50.8	6.3	.79	-.03	-.024	-.042	.00	-.097
60.9	4.8	1.08	-.22	-.109	-.045	.00	-.102
70.9	3.2	1.27	-.37	-.161	-.033	.00	-.072
80.8	1.6	1.31	-.46	-.199	-.019	.00	-.038
90.8	-.1	1.30	-.44	-.136	.002	.00	-.024
Model reversed							
89.0	-0.1	1.40	-0.53	-0.219	0.002	-0.01	0.055
99.2	1.6	.97	-.29	-.091	-.033	-.01	.007
109.0	3.2	.85	-.32	-.261	-.049	-.01	-.018
118.6	4.8	1.18	-.56	-.412	-.058	-.00	-.091
128.5	6.2	1.25	-.65	-.410	-.023	.01	-.080
138.7	7.5	1.03	-.61	-.353	-.029	.00	-.048
148.9	8.5	.85	-.57	-.323	-.045	.00	-.060
159.1	9.3	.71	-.56	-.314	-.051	.00	-.057
164.2	9.6	.65	-.55	-.304	-.049	.00	-.048
190.5	9.8	-.46	-.30	-.117	-.025	.01	-.085
200.8	9.3	-.73	-.34	-.133	-.025	.01	-.088
211.1	8.5	-.95	-.38	-.139	-.030	.01	-.096
221.2	7.5	-1.04	-.37	-.114	-.031	.01	-.102
231.3	6.2	-1.15	-.33	-.124	-.019	.00	-.060
241.3	4.8	-1.27	-.33	-.132	-.011	.00	-.031
251.2	3.2	-1.30	-.30	-.141	-.009	.00	-.025
261.1	1.5	-1.33	-.28	-.148	-.006	.00	-.016
271.0	-.1	-1.34	-.25	-.149	-.004	.00	-.005
Model forward							
269.3	-0.1	-1.36	-0.27	-0.162	0.009	-0.00	0.011
279.1	1.6	-1.34	-.23	-.160	.008	-.00	.002
288.9	3.2	-1.30	-.19	-.143	.005	-.00	-.009
298.9	4.8	-1.20	-.14	-.102	-.002	-.00	-.036
309.0	6.3	-.86	-.03	-.050	-.014	.00	-.068
319.2	7.6	-.56	.03	-.013	-.018	.00	-.076
324.3	8.1	-.44	.06	-.000	-.018	.00	-.076
329.4	8.6	-.32	.08	.010	-.018	.00	-.073
334.5	9.0	-.23	.08	.007	-.017	.00	-.068
339.6	9.3	-.15	.12	.024	-.016	.00	-.065
342.1	9.5	-.12	.12	.028	-.016	.00	-.063
344.7	9.6	-.09	.13	.030	-.016	-.00	-.062
347.2	9.7	-.07	.14	.034	-.015	-.00	-.061
349.7	9.8	-.05	.15	.038	-.015	.00	-.060
352.3	9.9	-.05	.16	.048	-.014	.00	-.061
354.8	9.9	-.03	.16	.050	-.015	.00	-.062
357.4	9.9	-.00	.16	.050	-.018	-.00	-.062
359.9	10.0	.00	.17	.054	-.018	.00	-.061

(c) $\phi = 30^{\circ}$

α, deg	β, deg	C_N	C_A	C_m	C_l	C_n	C_Y
Model forward							
2.8	30.1	0.04	0.18	0.066	-0.046	0.00	-0.169
5.7	30.0	.06	.19	.073	-.050	.00	-.177
8.6	29.8	.07	.19	.075	-.054	.00	-.185
11.5	29.6	.09	.19	.080	-.058	.00	-.190
14.4	29.3	.11	.20	.085	-.062	.00	-.196
17.2	29.0	.13	.20	.086	-.068	.00	-.206
20.0	28.6	.16	.19	.087	-.073	.00	-.216
22.8	28.2	.19	.19	.086	-.077	.00	-.225
28.4	27.1	.26	.16	.076	-.084	.01	-.237
33.8	25.8	.35	.13	.063	-.091	.01	-.253
39.1	24.4	.45	.09	.046	-.098	.01	-.265
44.3	22.8	.56	.04	.022	-.108	.01	-.283
54.3	19.1	.84	-.04	-.027	-.123	.01	-.303
63.8	14.9	1.13	-.26	-.127	-.108	.01	-.263
73.0	10.3	1.22	-.39	-.159	-.075	.01	-.177
81.8	5.4	1.28	-.48	-.199	-.048	.00	-.106
90.5	.4	1.26	-.43	-.128	-.003	.00	-.027
Model reversed							
91.4	1.8	1.42	-0.56	-0.240	-0.033	-0.02	0.034
106.9	10.3	1.01	-.39	-.258	-.130	-.02	-.114
125.4	19.2	1.16	-.57	-.346	-.072	.01	-.155
135.4	23.1	1.03	-.58	-.354	-.103	.04	-.253
145.9	26.1	.83	-.52	-.317	-.104	.02	-.233
156.9	28.3	.68	-.48	-.277	-.111	.01	-.235
168.3	29.8	.54	-.44	-.242	-.116	.03	-.262
180.0	30.2	-.02	-.21	-.082	-.043	.04	-.179
191.6	29.7	-.37	-.21	-.073	-.059	.02	-.213
203.0	28.3	-.62	-.24	-.067	-.050	.03	-.208
214.0	26.0	-.80	-.25	-.062	-.040	.02	-.189
224.5	22.9	-.95	-.27	-.081	-.036	.02	-.160
234.5	19.2	-1.14	-.27	-.083	-.037	.02	-.140
253.1	10.4	-1.36	-.28	-.119	-.015	.00	-.070
268.5	1.8	-1.42	-.25	-.137	-.005	-.00	-.023
Model forward							
269.5	0.5	-1.3170	-0.25	-0.160	0.009	0.00	0.012
278.1	5.4	-1.2947	-.21	-.153	.005	.00	-.015
286.9	10.3	-1.2400	-.17	-.138	-.002	.00	-.055
296.1	14.8	-1.1143	-.12	-.107	-.021	.00	-.118
305.6	19.0	-.8480	-.02	-.047	-.043	.00	-.189
315.6	22.8	-.5762	.06	-.004	-.057	.00	-.223
320.8	24.4	-.4544	.09	.011	-.056	.00	-.215
326.1	25.8	-.3531	.11	.024	-.052	.00	-.200
331.5	27.1	-.2669	.13	.035	-.046	.00	-.185
337.1	28.2	-.1929	.15	.043	-.045	.00	-.180
339.9	28.6	-.1588	.16	.047	-.046	.00	-.182
342.7	29.0	-.1275	.17	.052	-.044	.00	-.174
345.6	29.3	-.1036	.18	.056	-.044	.00	-.173
348.4	29.6	-.0900	.18	.061	-.044	.00	-.174
351.3	29.8	-.0533	.18	.058	-.047	.00	-.171
354.2	30.0	-.0339	.19	.062	-.046	.00	-.167
357.1	30.1	-.0171	.19	.067	-.048	.00	-.170
360.0	30.1	.0066	.20	.069	-.050	.00	-.174

TABLE I.- BASIC AERODYNAMIC DATA AT M = 4.5 - Continued

(d) $\phi = 60^{\circ}$

α, deg	β, deg	C_N	C_A	C_m	C_l	C_n	C_Y
Model forward							
0.0	60.2	-0.00	0.15	0.063	-0.068	0.00	-0.2564
5.0	60.0	.03	.15	.061	-.065	.00	-.2483
9.9	59.8	.04	.15	.064	-.073	.00	-.2656
14.8	59.3	.07	.15	.065	-.079	.00	-.2766
19.5	58.7	.10	.15	.066	-.085	.00	-.2902
23.9	57.9	.13	.14	.065	-.090	.00	-.3006
28.2	57.0	.16	.13	.062	-.096	.01	-.3178
32.3	55.9	.21	.13	.059	-.103	.01	-.3314
36.1	54.7	.25	.11	.054	-.112	.01	-.3503
43.1	52.0	.35	.08	.037	-.131	.01	-.3834
49.2	48.9	.46	.04	.018	-.153	.01	-.4281
54.6	45.6	.57	-.00	.001	-.177	.01	-.4725
59.3	42.0	.67	-.06	-.023	-.196	.01	-.4991
67.3	34.3	.89	-.20	-.086	-.177	.00	-.4252
73.9	26.2	1.09	-.33	-.150	-.135	.00	-.3276
79.7	17.9	1.26	-.42	-.194	-.103	.00	-.2361
85.0	9.3	1.24	-.45	-.177	-.088	-.01	-.1556
90.0	.7	1.20	-.40	-.109	-.020	-.01	-.0076
Model reversed							
91.2	3.1	1.38	-0.47	-0.222	-0.058	-0.01	-0.0865
94.9	9.5	1.22	-.46	-.209	-.136	-.01	-.2046
100.2	18.1	1.18	-.46	-.243	-.122	-.00	-.2212
106.0	26.5	1.12	-.48	-.268	-.130	.01	-.2623
112.7	34.6	.94	-.40	-.219	-.147	.01	-.3200
120.7	42.2	.75	-.33	-.171	-.140	.01	-.3149
125.5	45.7	.66	-.30	-.155	-.132	.02	-.3052
130.9	49.1	.58	-.28	-.150	-.128	.02	-.3028
137.0	52.2	.52	-.27	-.145	-.127	.02	-.3061
144.0	54.9	.46	-.25	-.137	-.130	.03	-.3187
147.8	56.1	.42	-.24	-.128	-.131	.03	-.3268
151.9	57.2	.38	-.22	-.118	-.133	.03	-.3352
156.2	58.1	.33	-.20	-.108	-.132	.03	-.3414
160.7	58.9	.29	-.18	-.092	-.127	.03	-.3373
165.3	59.5	.24	-.17	-.081	-.124	.03	-.3385
170.2	60.0	.21	-.16	-.073	-.122	.03	-.3384
174.8	60.1	-.04	-.03	.001	-.060	.03	-.2578
179.8	60.2	-.10	-.03	.001	-.058	.03	-.2584
184.8	60.2	-.14	-.04	-.002	-.058	.03	-.2611
189.7	59.9	-.19	-.04	-.004	-.058	.03	-.2660
194.5	59.5	-.24	-.05	-.007	-.059	.03	-.2747
199.2	58.9	-.29	-.06	-.010	-.060	.02	-.2832
203.7	58.1	-.33	-.07	-.014	-.060	.03	-.2921
208.0	57.2	-.38	-.07	-.012	-.062	.02	-.3036
212.0	56.1	-.42	-.08	-.015	-.062	.03	-.3088
215.9	54.9	-.47	-.09	-.017	-.066	.03	-.3246
222.8	52.2	-.54	-.10	-.016	-.059	.03	-.3082
229.0	49.1	-.62	-.10	-.022	-.055	.02	-.2896
234.3	45.8	-.71	-.12	-.032	-.055	.02	-.2758
239.1	42.2	-.81	-.14	-.048	-.053	.02	-.2568
247.1	34.6	-1.00	-.18	-.076	-.035	.01	-.2016
253.8	26.5	-1.18	-.21	-.102	-.029	.01	-.1543
259.6	18.2	-1.30	-.23	-.117	-.022	.00	-.1055
264.9	9.6	-1.35	-.24	-.127	-.013	.00	-.0595
268.7	3.1	-1.36	-.23	-.128	-.006	-.00	-.0206
Model forward							
270.0	0.6	-1.30	-0.26	-0.159	0.013	-0.00	0.0343
275.0	9.3	-1.28	-.24	-.161	.006	-.00	-.0136
280.3	17.9	-1.22	-.21	-.151	-.008	.00	-.0791
286.0	26.2	-1.10	-.16	-.126	-.026	.00	-.1546
292.7	34.3	-.92	-.09	-.091	-.049	.00	-.2435
300.7	42.0	-.72	-.02	-.043	-.080	.01	-.3366
305.5	45.6	-.62	-.00	-.030	-.086	.01	-.3447
310.8	48.9	-.51	.04	.001	-.084	.01	-.3293
316.9	52.0	-.39	.07	.015	-.078	.00	-.3105
323.9	54.7	-.28	.10	.029	-.073	.00	-.2974
327.7	55.9	-.24	.11	.035	-.072	.00	-.2892
331.8	57.0	-.20	.12	.042	-.069	.00	-.2811
336.1	57.9	-.16	.14	.048	-.065	.00	-.2679
340.6	58.7	-.13	.14	.053	-.064	.00	-.2599
345.2	59.3	-.09	.13	.047	-.062	.00	-.2514
350.1	59.8	-.07	.16	.064	-.061	.00	-.2456
355.0	60.1	-.04	.17	.067	-.065	.00	-.2503

TABLE I.- BASIC AERODYNAMIC DATA AT M = 4.5 - Continued

(e) $\phi = 87°$

α, deg	β, deg	C_N	C_A	C_m	C_l	C_n	C_Y
Model forward							
0.0	87.0	-0.01	0.04	0.020	-0.059	0.01	-0.235
40.7	86.1	.02	.03	.019	-.063	.01	-.239
59.8	84.2	.03	.03	.015	-.068	.01	-.252
68.9	81.9	.06	.02	.014	-.070	.01	-.259
74.0	79.6	.10	.02	.013	-.075	.01	-.271
77.1	77.1	.14	.01	.010	-.082	.01	-.287
79.3	74.7	.18	.00	.003	-.088	.01	-.302
80.9	72.2	.24	-.00	-.001	-.095	.01	-.318
82.1	69.8	.30	-.02	-.008	-.103	.01	-.333
83.9	64.8	.43	-.05	-.027	-.125	.01	-.375
85.0	59.8	.55	-.10	-.043	-.147	.01	-.407
85.9	54.9	.69	-.15	-.071	-.174	.01	-.447
86.6	49.9	.80	-.22	-.106	-.195	.00	-.470
87.6	39.9	.96	-.31	-.165	-.191	.01	-.415
88.3	29.9	1.11	-.42	-.218	-.150	.01	-.319
88.9	19.9	1.20	-.44	-.225	-.126	.00	-.234
89.5	9.9	1.22	-.46	-.198	-.127	-.02	-.160
89.9	2.5	1.22	-.43	-.149	-.053	-.03	.012
Model reversed							
90.1	2.5	1.45	-0.49	-0.247	-0.041	0.00	-0.111
90.5	9.9	1.31	-.39	-.178	-.095	-.00	-.197
91.0	19.9	1.24	-.36	-.181	-.117	.00	-.233
91.6	29.9	1.13	-.34	-.176	-.152	.01	-.339
92.2	39.9	.98	-.26	-.135	-.196	.02	-.447
93.2	49.9	.82	-.18	-.086	-.198	.01	-.482
93.8	54.9	.72	-.12	-.057	-.172	.01	-.447
94.7	59.8	.59	-.08	-.037	-.146	.01	-.405
95.8	64.8	.46	-.05	-.019	-.126	.01	-.372
97.5	69.8	.33	.00	.005	-.105	.02	-.332
98.7	72.2	.27	-.01	-.004	-.099	.02	-.322
100.3	74.7	.22	-.00	.001	-.095	.02	-.314
102.3	77.2	.17	.00	.002	-.089	.02	-.300
105.4	79.6	.13	.01	.010	-.085	.02	-.291
110.2	82.0	.09	.02	.014	-.085	.02	-.293
119.2	84.2	.06	.03	.024	-.075	.02	-.274
138.3	86.2	.03	.03	.023	-.071	.02	-.265
180.0	87.1	-.00	.03	.019	-.068	.02	-.259
221.5	86.2	-.04	.02	.017	-.065	.02	-.257
240.6	84.2	-.07	.02	.016	-.064	.02	-.254
249.4	81.9	-.12	.02	.012	-.063	.01	-.254
254.4	79.6	-.15	.00	.006	-.071	.02	-.273
257.5	77.2	-.21	.00	.000	-.077	.02	-.289
259.7	74.7	-.26	.00	.000	-.077	.02	-.295
261.2	72.2	-.32	-.00	-.005	-.082	.02	-.307
262.4	69.8	-.37	-.01	-.011	-.085	.02	-.325
264.0	64.8	-.49	-.04	-.029	-.091	.02	-.332
265.2	59.8	-.60	-.06	-.042	-.095	.02	-.342
266.0	54.9	-.72	-.08	-.055	-.089	.02	-.337
266.7	49.9	-.82	-.11	-.066	-.085	.02	-.334
267.6	39.9	-1.00	-.16	-.091	-.052	.01	-.258
268.3	29.9	-1.17	-.20	-.113	-.035	.00	-.180
268.9	19.9	-1.30	-.23	-.128	-.023	.00	-.112
269.5	9.9	-1.35	-.24	-.133	-.012	-.00	-.050
269.9	2.5	-1.37	-.24	-.132	-.007	-.00	-.012
Model forward							
270.1	2.5	-1.38	-0.28	-0.146	0.000	0.00	-0.004
270.5	9.9	-1.35	-.28	-.145	-.003	.00	-.039
271.0	19.9	-1.29	-.26	-.138	-.014	.01	-.097
271.6	29.9	-1.15	-.22	-.122	-.022	.01	-.156
272.4	39.9	-.99	-.17	-.096	-.040	.01	-.236
273.4	49.9	-.81	-.11	-.068	-.075	.02	-.319
274.1	54.9	-.72	-.08	-.055	-.082	.02	-.330
274.9	59.8	-.60	-.06	-.041	-.086	.02	-.331
276.1	64.8	-.49	-.04	-.026	-.088	.02	-.327
277.8	69.8	-.37	-.02	-.012	-.082	.02	-.311
279.0	72.2	-.31	-.01	-.008	-.077	.01	-.297
280.7	74.7	-.26	-.00	-.003	-.073	.01	-.283
282.8	77.1	-.21	.00	.000	-.067	.01	-.267
286.0	79.5	-.17	.01	.005	-.064	.01	-.256
291.0	81.9	-.12	.02	.009	-.059	.01	-.242
300.1	84.2	-.09	.03	.014	-.061	.01	-.243
319.3	86.1	-.05	.04	.019	-.059	.01	-.235

TABLE I.- BASIC AERODYNAMIC DATA AT $M = 4.5$ - Concluded

(f) $\phi = 90^{\circ}$

α, deg	β, deg	C_N	C_A	C_m	C_l	C_n	C_Y
Model forward							
90.0	0.0	1.15	-0.38	-0.096	-0.003	-0.00	-0.023
90.0	10.0	1.20	-.48	-.178	-.117	-.03	-.143
90.0	20.0	1.19	-.45	-.213	-.133	-.00	-.253
90.1	30.0	1.10	-.47	-.221	-.166	.01	-.356
90.1	40.0	.95	-.36	-.172	-.194	.01	-.437
90.3	50.0	.79	-.28	-.123	-.213	.00	-.512
90.3	55.0	.71	-.20	-.082	-.195	.00	-.496
90.3	60.0	.58	-.14	-.049	-.162	.00	-.442
90.3	65.0	.46	-.09	-.034	-.139	.01	-.410
90.4	70.0	.33	-.05	-.015	-.116	.01	-.365
90.4	72.5	.27	-.03	-.010	-.107	.01	-.347
90.5	75.0	.21	-.02	-.007	-.099	.01	-.328
90.5	77.5	.16	-.01	-.003	-.092	.01	-.315
90.6	80.0	.12	-.00	-.000	-.086	.01	-.300
90.8	82.5	.09	-.00	.001	-.079	.01	-.286
91.1	85.0	.05	.00	.005	-.076	.01	-.279
92.2	87.5	.02	.00	.007	-.074	.01	-.272
0 to 360.0	90.0	-.00	.02	.014	-.068	.01	-.260
267.9	87.5	-.02	.02	.014	-.067	.01	-.253
268.9	85.0	-.08	.02	.013	-.059	.01	-.242
269.3	82.5	-.11	.02	.008	-.057	.01	-.241
269.5	80.0	-.15	.01	.002	-.061	.01	-.256
269.5	77.5	-.19	.00	-.001	-.065	.01	-.268
269.6	75.0	-.24	-.03	-.019	-.069	.01	-.281
269.7	72.5	-.29	-.01	-.014	-.074	.01	-.296
269.7	70.0	-.35	-.05	-.031	-.080	.02	-.315
269.7	65.0	-.46	-.04	-.035	-.087	.02	-.332
269.8	60.0	-.56	-.06	-.054	-.083	.02	-.327
269.8	55.0	-.67	-.09	-.071	-.082	.01	-.326
269.9	50.0	-.76	-.12	-.086	-.078	.01	-.324
269.9	40.0	-.93	-.17	-.113	-.047	.01	-.251
270.0	30.0	-1.08	-.22	-.143	-.028	.00	-.170
270.0	20.0	-1.23	-.26	-.164	-.014	.00	-.093
270.0	10.0	-1.29	-.28	-.170	.002	.00	-.020
270.0	.0	-1.32	-.29	-.170	.011	-.00	.034

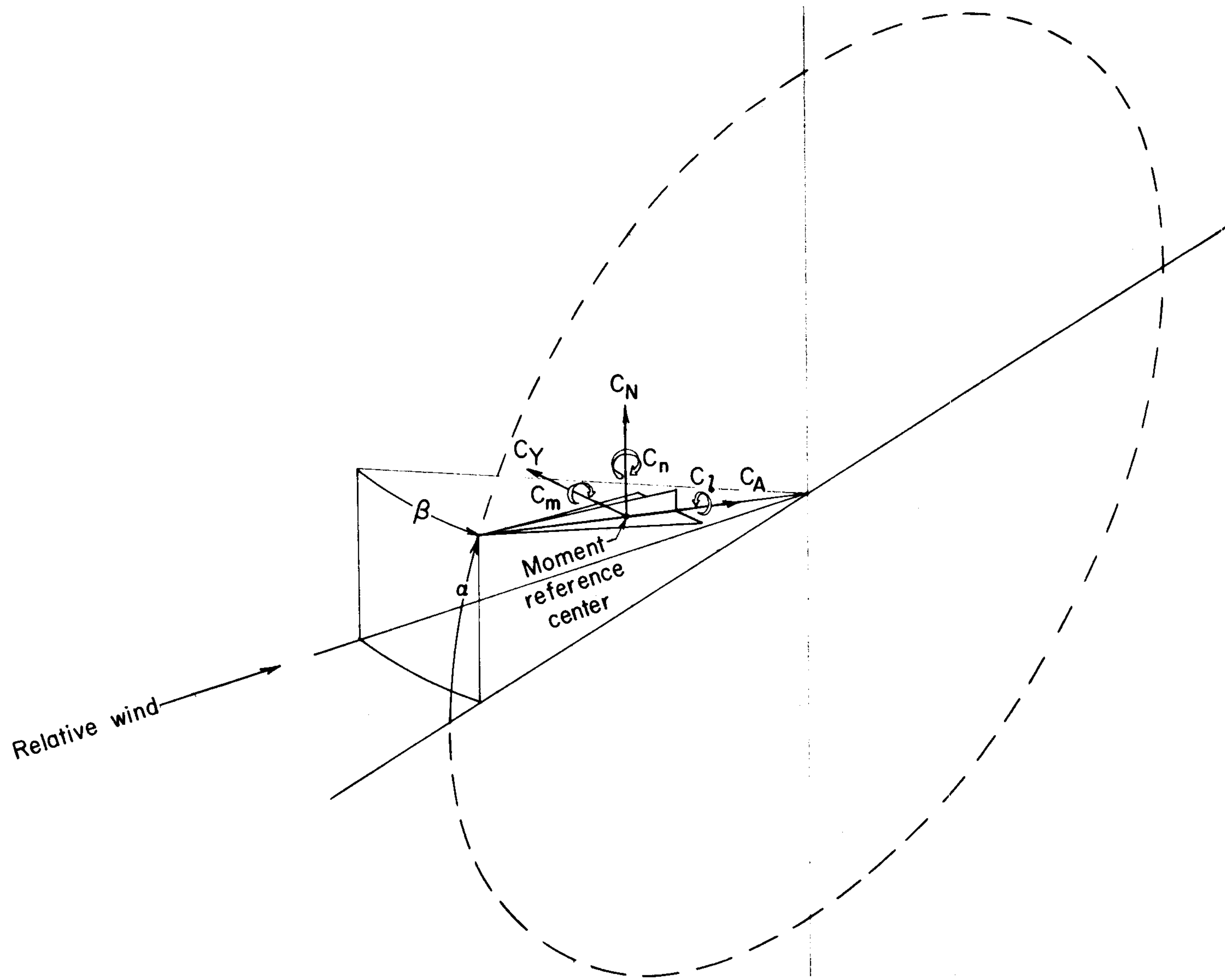

Figure 1.- System of axes. Arrows denote positive directions of forces, moments, and angular measurements.

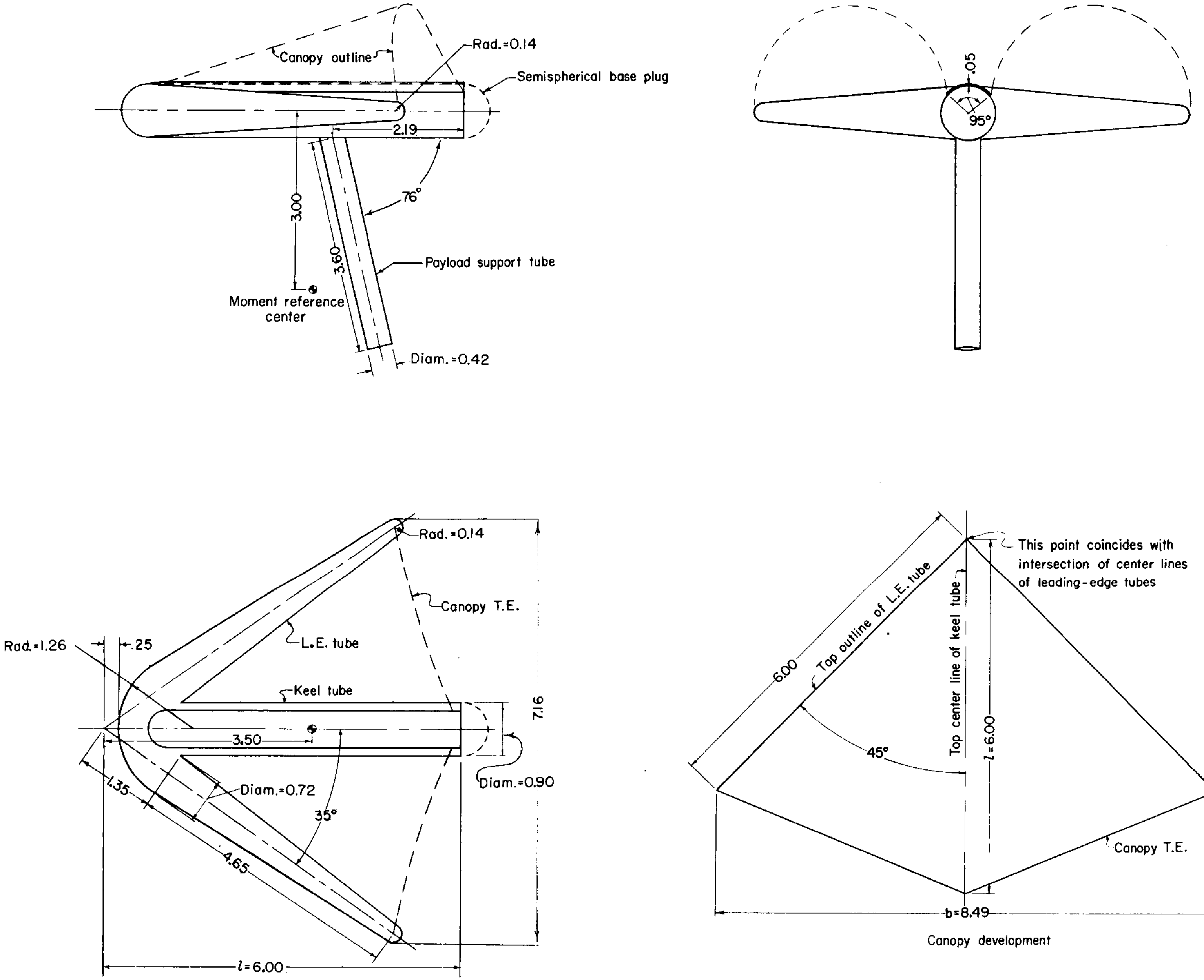

Figure 2.- Details of the paraglider model. All dimensions are in inches unless otherwise noted.

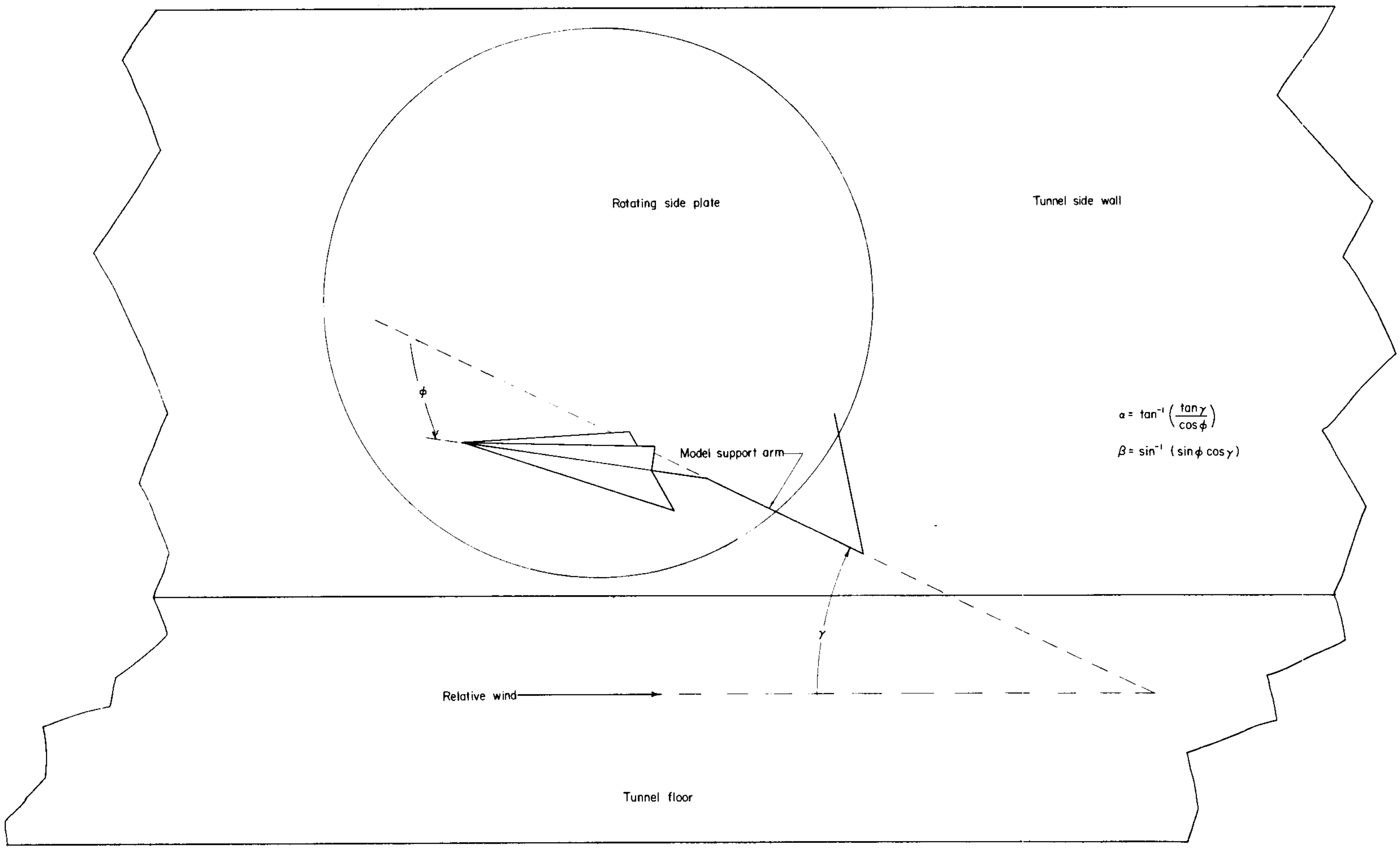

Figure 3.- Schematic diagram of model support system.

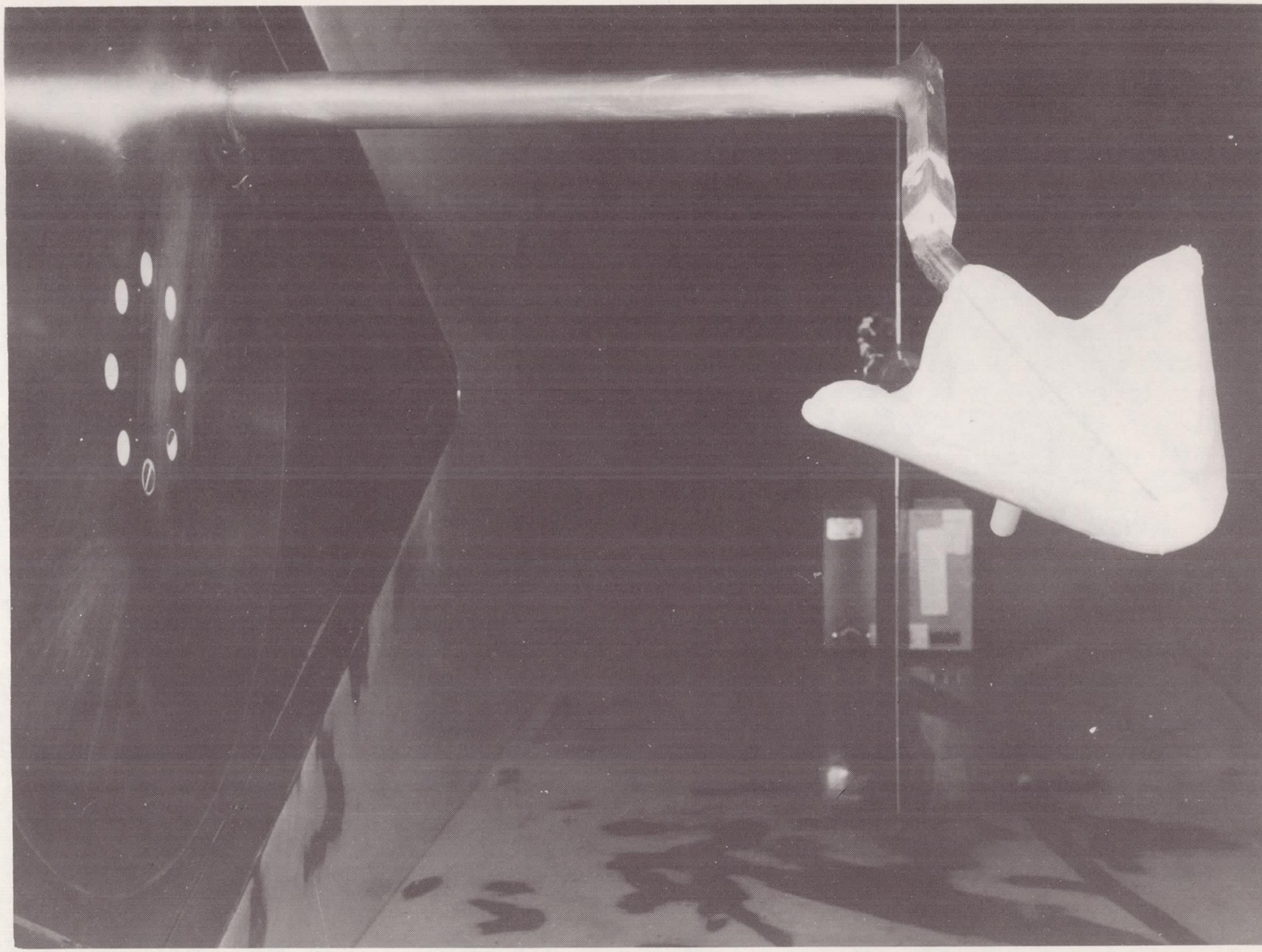

(a) Model facing forward on the support system. L-62-3266

Figure 4.- Model mounted in the 2-foot hypersonic facility at the Langley Research Center.

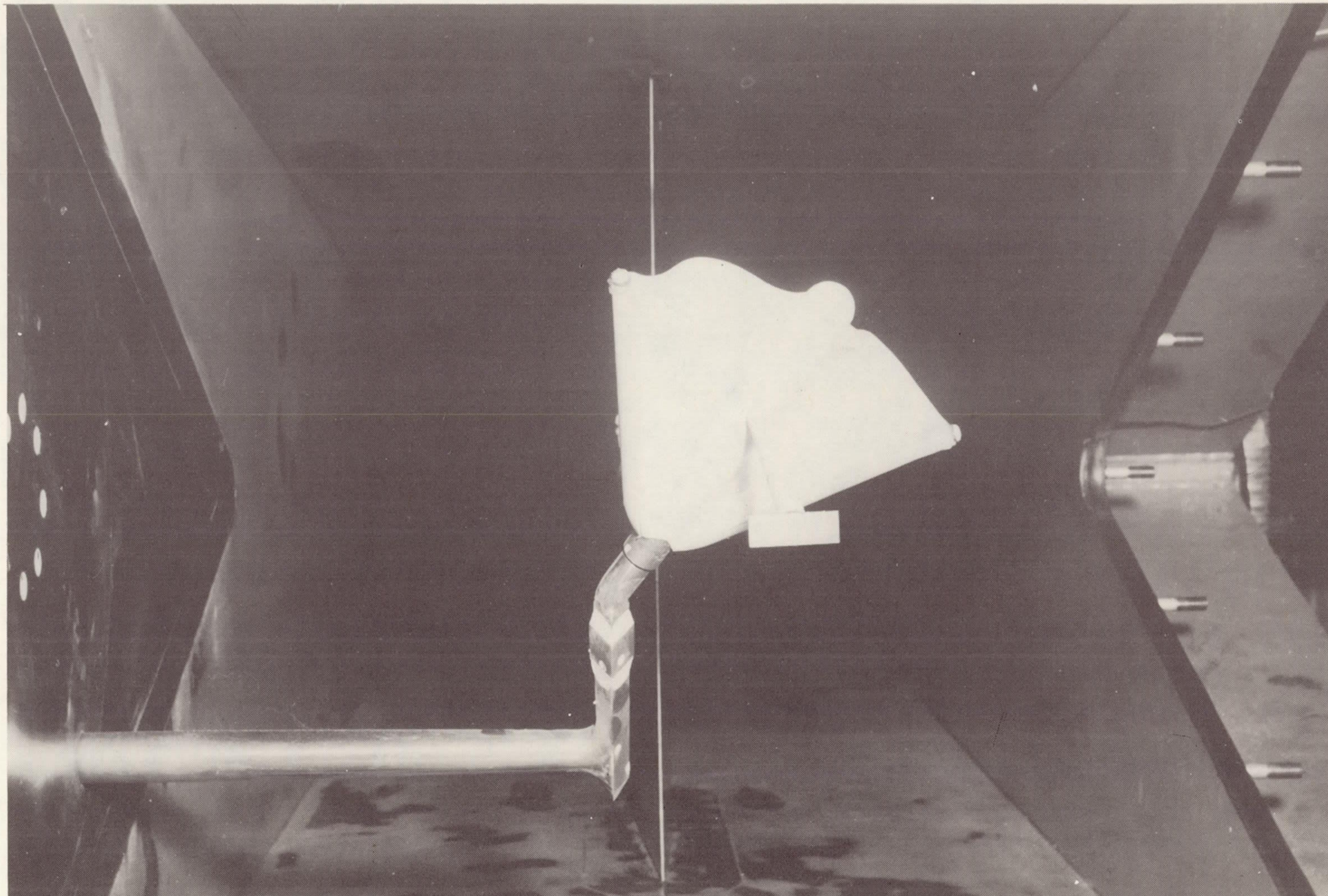

(b) Model facing rearward on the support system. L-62-3056

Figure 4.- Concluded.

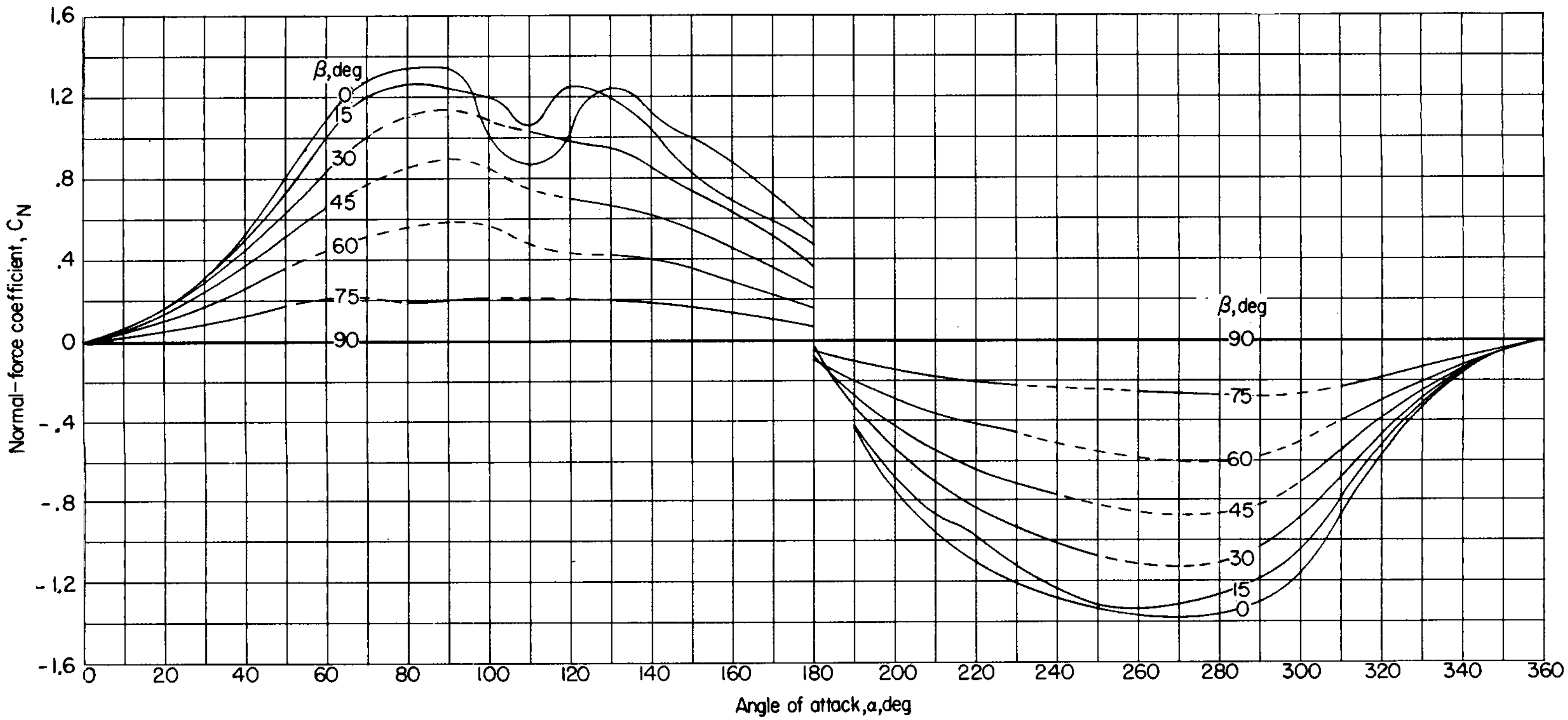

(a) Normal-force coefficient.

Figure 5.- Variation of the aerodynamic coefficients of the paraglider model with angle of attack at constant sideslip angles for a Mach number of 4.5.

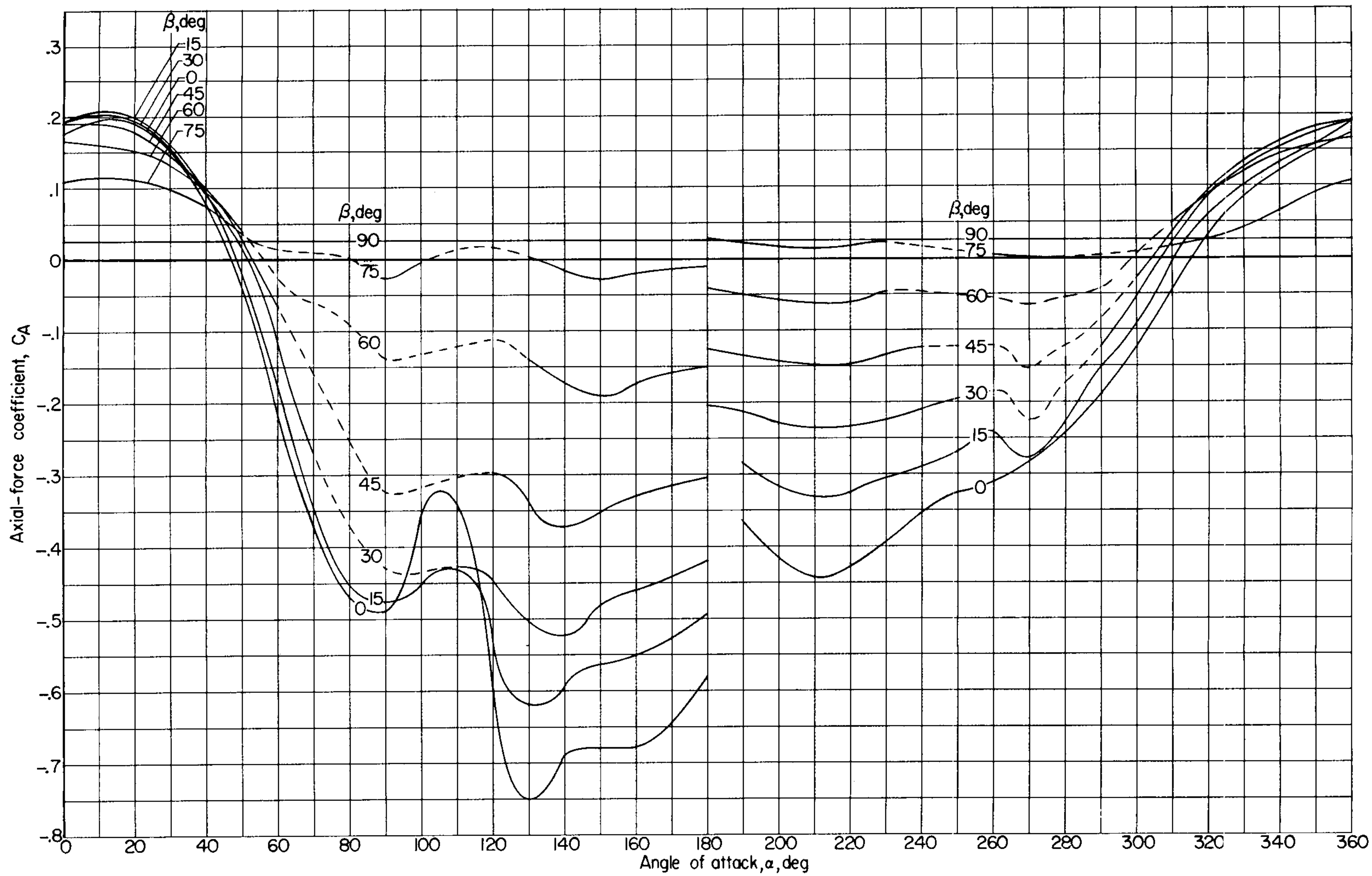

(b) Axial-force coefficient.

Figure 5.- Continued.

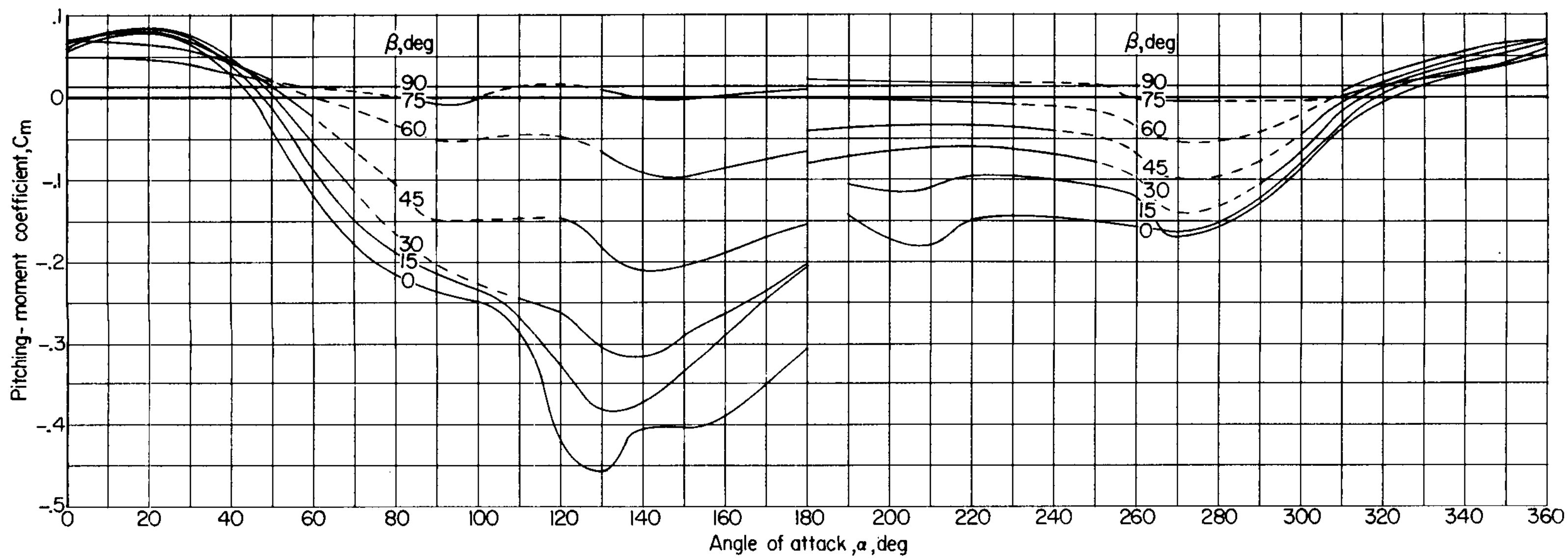

(c) Pitching-moment coefficient.

Figure 5.- Continued.

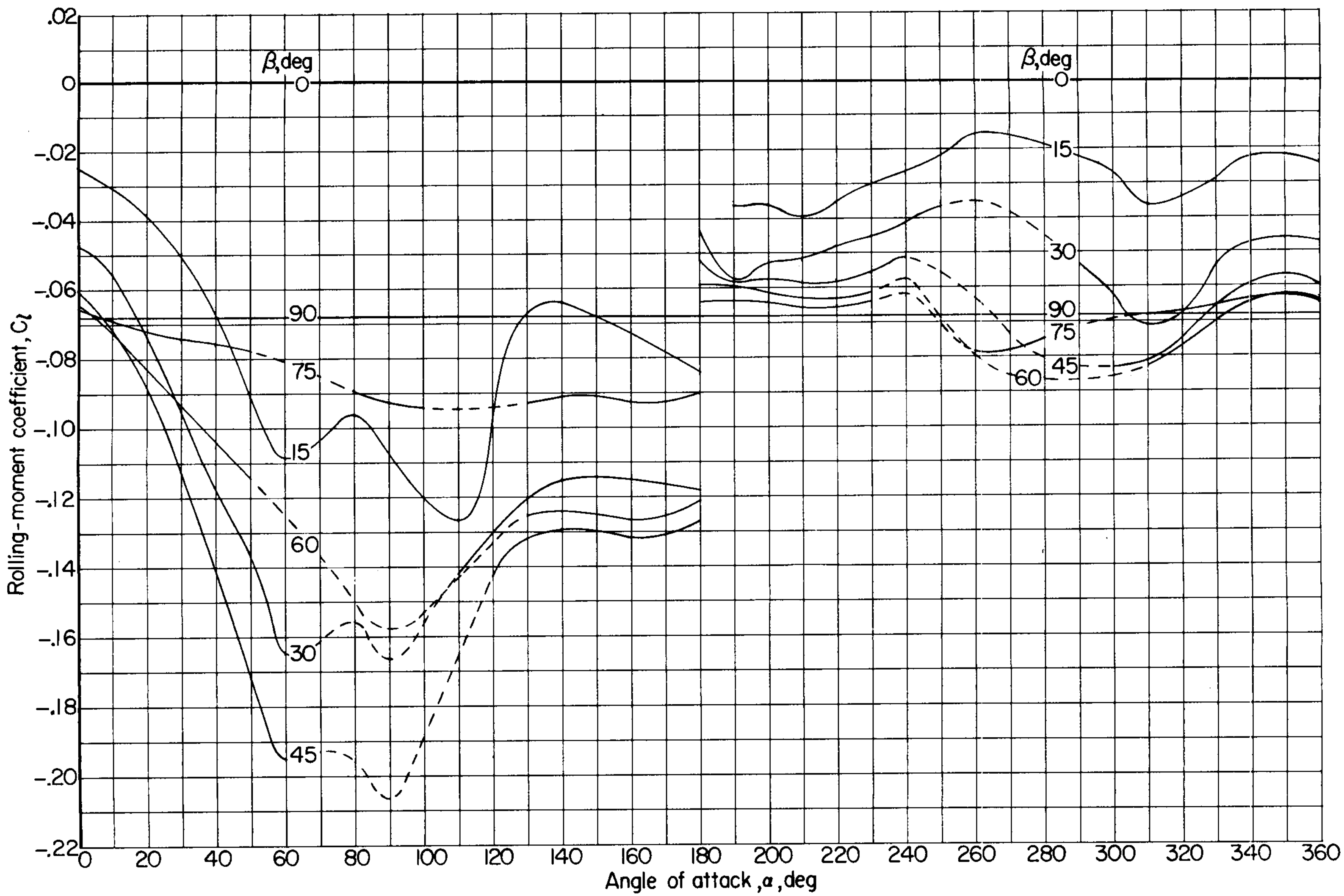

(d) Rolling-moment coefficient.

Figure 5.- Continued.

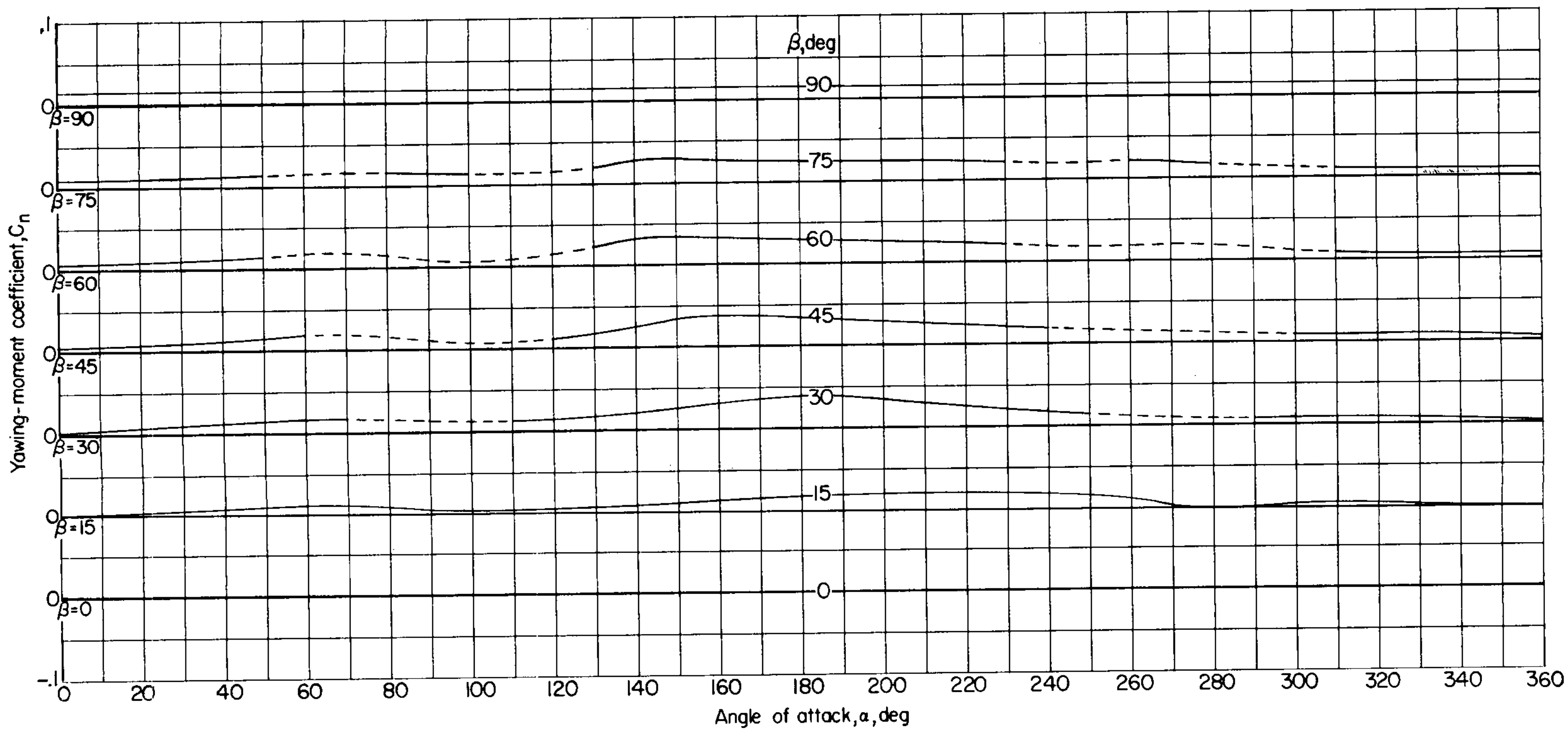

(e) Yawing-moment coefficient.

Figure 5.- Continued.

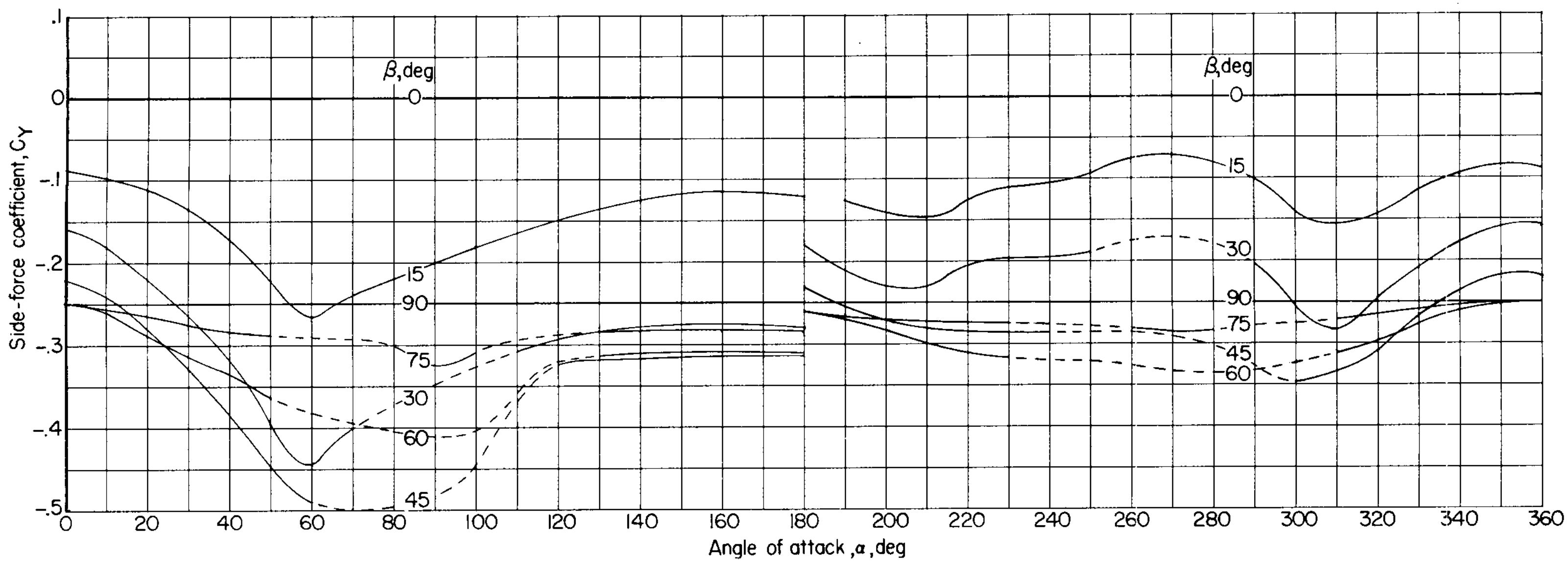

(f) Side-force coefficient.

Figure 5.- Concluded.

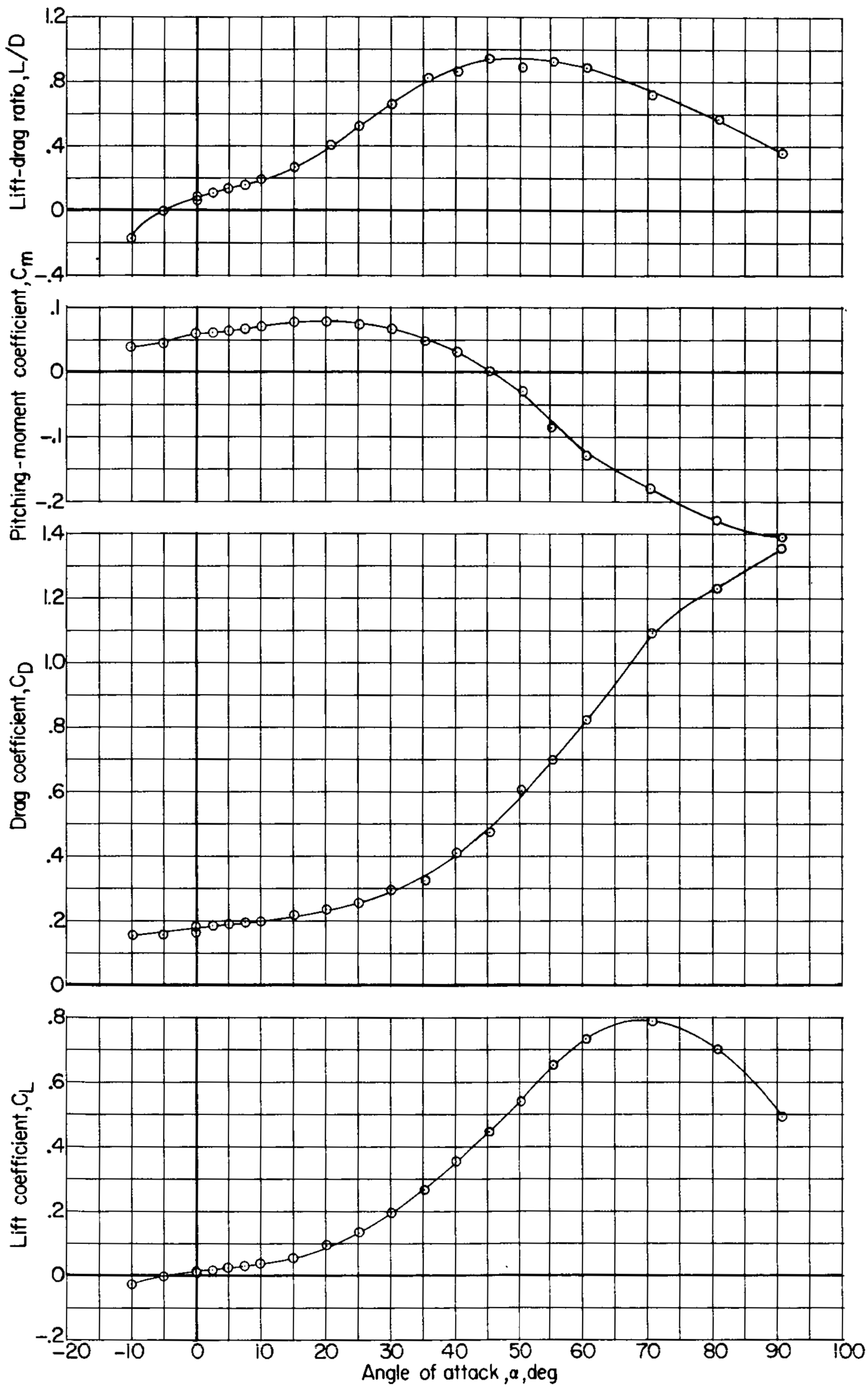

Figure 6.- Longitudinal aerodynamic characteristics of the paraglider model at a Mach number of 4.5. $\beta = 0^{\circ}$.